Anti–Prostate-Specific Membrane Antigen Liposomes Loaded with ^{225}Ac for Potential Targeted Antivascular α-Particle Therapy of Cancer

Amey Bandekar[1], Charles Zhu*[1], Rohit Jindal*[1], Frank Bruchertseifer[2], Alfred Morgenstern[2], and Stavroula Sofou[1]

[1]*Departments of Chemical and Biochemical Engineering and Biomedical Engineering, Rutgers University, Piscataway, New Jersey; and* [2]*Alpha-Immunotherapy, European Commission, Joint Research Centre, Institute for Transuranium Elements, Karlsruhe, Germany*

This study evaluates targeted liposomes loaded with the α-particle generator ^{225}Ac to selectively kill prostate-specific membrane antigen (PSMA)–expressing cells with the aim to assess their potential for targeted antivascular radiotherapy. **Methods:** In this study, PEGylated liposomes were loaded with ^{225}Ac and labeled with the mouse antihuman PSMA J591 antibody or with the A10 PSMA aptamer. The targeting selectivity, extent of internalization, and killing efficacy of liposomes were evaluated on monolayers of prostate cancer cells intrinsically expressing PSMA (human LNCaP and rat Mat-Lu cells) and on monolayers of HUVEC induced to express PSMA (induced HUVEC). **Results:** The loading efficiency of ^{225}Ac into preformed liposomes ranged from 58.0% ± 4.6% to 85.6% ± 11.7% of introduced radioactivity. The conjugation reactions resulted in approximately 17 ± 2 J591 antibodies and 9 ± 2 A10 aptamers per liposome. The average size of liposomes, 107 ± 2 nm in diameter, was not affected by conjugation or loading. LNCaP cells exhibit 2:1:0.5 relative PSMA expression, compared with MatLu and induced HUVEC, respectively, based on flow cytometry detecting association of the J591 antibody. J591-labeled liposomes display higher levels of total specific binding to all cell lines than A10 aptamer-labeled liposomes. Specific cell association of targeted liposomes increases with incubation time. Cytotoxicity studies demonstrate that radiolabeled J591-labeled liposomes are most cytotoxic, with median lethal dose values, after 24 h of incubation, equal to 1.96 (5.3×10^{-5}), 2.92×10^{2} (7.9×10^{-3}), and 2.33×10^{1} Bq/mL (6.3×10^{-4} μCi/mL) for LNCaP, Mat-Lu, and induced HUVEC, respectively, which are comparable to the values for the radiolabeled J591 antibody. For A10 aptamer–labeled liposomes, the corresponding values are 3.70×10^{1} (1.0×10^{-3}), 1.85×10^{3} (5.0×10^{-2}), and 4.07×10^{3} Bq/mL (1.1×10^{-1} μCi/mL), respectively. **Conclusion:** Our studies demonstrate that anti-PSMA–targeted liposomes loaded with ^{225}Ac selectively bind, become internalized, and kill PSMA-expressing cells including endothelial cells induced to express PSMA. These findings—combined with the unique ability of liposomes to be easily tuned, in terms of size and surface modification, for optimizing biodistributions—suggest the potential of PSMA-targeting liposomes encapsulating α-particle emitters for selective antivascular α radiotherapy.

Key Words: anti-PSMA liposomes; liposomal ^{225}Ac; antivascular α-particle radiotherapy

J Nucl Med 2014; 55:107–114
DOI: 10.2967/jnumed.113.125476

The development of vasculature is needed for solid tumors to grow beyond 1–2 mm^3 (*1*), and antivascular therapy aims to damage and kill tumor cells by cutting the blood flow via the neovasculature, depriving the tumor of growth factors (*2*). Without adequate vasculature, tumor cells are shown to become necrotic or apoptotic (*3*). Within this framework, epitopes exclusively expressed by the tumor endothelium have been identified, and targeting molecules have been developed and demonstrated the ability to selectively target the tumor neovasculature. Powerful therapeutics such as α-particle emitters have been suggested as ideal because of their high energy and short range, resulting in high killing efficacies and low irradiation of the surrounding healthy tissues (*4*). However, the absence of a targeted therapeutic modality that combines fast and selective delivery of lethal doses to tumor neovasculature and exhibits rapid removal from circulation to keep toxicities at a minimum still holds.

In this study, we aim to address the selectivity part of the above challenges by following a bottom-up design, which includes 3 base elements. First, the targeting receptor is chosen to be the prostate-specific membrane antigen (PSMA), and 2 different targeting ligands—an antibody and an aptamer—are evaluated. Second, as the therapeutic radionuclide, the atomic-sized α-particle generator ^{225}Ac is used, and third, the delivery vehicle is a self-assembled nanometer-sized liposome. The rationale for these choices is briefly described below.

Studies on patients with different types of primary tumors report selective expression of PSMA by the tumor neovasculature (*5,6*). The absence of PSMA on the endothelium of healthy tissues may enable, therefore, the targeting of vascular PSMA to potentially become a therapeutic strategy for selective delivery of drugs to the tumor vasculature. In this study, we evaluated 2 different targeting ligands. The first ligand was the anti-PSMA monoclonal antibody J591, which binds to the extracellular domain of PSMA with high affinity and is also rapidly internalized (*6,7*). In a phase I trial, J591 was shown to specifically target the tumor neovasculature in humans bearing multiple solid tumor types (*8*), a finding that

Received Sep. 10, 2013; revision accepted Sep. 24, 2013.
For correspondence or reprints contact: Stavroula Sofou, Departments of Chemical and Biochemical Engineering and Biomedical Engineering, Rutgers University, 599 Taylor Road, Piscataway, NJ 08854.
E-mail: ss1763@rci.rutgers.edu
*Contributed equally to this work.
Published online Dec. 12, 2013.

renders J591 and PSMA a unique ligand–receptor pair for selective in vivo targeting of the neovasculature of different types of cancer. We also evaluate the A10 PSMA aptamer, which has been designed to identify the extracellular domain of PSMA (*9*), is shown to target PSMA-expressing cells when conjugated on the surface of nanometer-sized particles (*10*), and is commercially available.

Second, as a therapeutic radionuclide, we chose an α-particle emitter because of the high cytotoxicity of α particles and their potential antivascular effect (*4*). The killing efficacy of α particles is independent of the cell oxygenation state or cell cycle during irradiation, and only a few tracks across the nucleus result in cell death (*11–14*) due to their high energy deposited per unit distance traveled (high linear energy transfer), which is approximately 80 keV/μm. In addition, their short range, 50–100 μm, allows for localized irradiation of targeted cells with minimal exposure of surrounding healthy tissues. We chose the atomic-sized α-particle generator ^{225}Ac, which decays with a 10-d half-life and generates 3 α-particle–emitting daughters (^{221}Fr [half-life, 4.9 min], ^{217}At [half-life, 32.3 ms], and ^{213}Bi [half-life, 45.6 min]), generating 4 α particles per ^{225}Ac decay.

However, although the retention of ^{225}Ac daughters at the target increases efficacy, escape and distribution throughout the body increases toxicity (*15*). During circulation, radiolabeled antibodies and other nanocarriers (up to 100 nm) (*16*) loaded with ^{225}Ac cannot retain any of the daughters because the bond between the chelate holding the radionuclide may be broken on transformation of the parent into the new daughter. As a result, daughters are released in the circulation and accumulate at the kidneys. Renal toxicity caused by escaped radioactive daughters of ^{225}Ac is still a challenge (*15*).

To address the above issues, we followed a liposome-based strategy to potentially deliver ^{225}Ac at the tumor neovasculature that will ultimately combine 2 critical properties. The first property is the fast binding and intracellular localization to extensively retain radioactive daughters within the targeted tumor endothelial cells, and the second is rapid sequestration of ^{225}Ac-loaded liposomal carriers, followed by their accumulation in less radiosensitive sites, such as the spleen (*17*), to spare radiosensitive kidneys from escaped daughters.

The objective of this study was to develop anti-PSMA liposomes encapsulating the α-particle generator ^{225}Ac for selective targeting of PSMA-expressing cells and to evaluate their potential for targeted antivascular radiotherapy. We have previously shown that these liposomes can be stably loaded with high radioactivities of ^{225}Ac (*18*). In this study, we compared the targeting selectivity and killing efficacy of liposomes labeled with the mouse antihuman PSMA J591 antibody (*6*) and with the A10 PSMA aptamer (*10*) on monolayers of cells, which either intrinsically express variable levels of PSMA or are induced to express PSMA. The first category of cell lines includes the PSMA-expressing LNCaP prostate cancer human cells, which are used as a positive control in our studies, and the PSMA-expressing Mat-Lu prostate cancer rat cells. The latter are mainly aimed to be used in our subsequent in vivo studies because of their vasculogenic mimicry (*19*) and will, therefore, be used as in vivo surrogates of tumor vasculature. The second category of cell line includes monolayers of HUVEC, which are induced to express PSMA (*20*) (induced HUVEC) because this cell line represents a closer analog to the tumor endothelium of interest.

MATERIALS AND METHODS

All materials are described in the supplemental data (supplemental materials are available at http://jnm.snmjournals.org).

Liposome Preparation and Radiolabeling with ^{225}Ac

Liposomes were composed of 1,2-dinonadecanoyl-sn-glycero-3-phosphocholine (DNPC):cholesterol:1,2-distearoyl-sn-glycero-3-phosphoethanolamine-*N*-[methoxy(polyethyleneglycol)-2000] (ammonium salt) (DSPE-PEG):1,2-dipalmitoyl-sn-glycero-3-phosphoethanolamine-*N*-(lissamine rhodamine B sulfonyl) (ammonium salt) (DPPE-rhodamine) at the mole ratio of 6.61:2.83:0.47:0.09 and were prepared to encapsulate citrate buffer and DOTA using the lipid hydration method (detailed methods are given in the supplemental data) (*18*). The size distribution of liposome suspensions was measured using a Zetasizer NanoSeries (Malvern Instruments Ltd.).

^{225}Ac was loaded into preformed liposomes encapsulating DOTA as described before (*18*). Loading was mediated by the A23187 ionophore by heating the liposome suspension in 4-(2-hydroxyethyl)-1-piperazineethanesulfonic acid (HEPES) buffer above the transition temperature of the lipid membrane (65°C–67°C). On completion of loading, and addition of DTPA, ^{225}Ac-loaded liposomes were purified by size-exclusion chromatography, and the loading efficiency of ^{225}Ac was determined by measuring the radioactivity of liposome suspensions before and after size-exclusion chromatography by counting the γ emissions of ^{213}Bi decay on reaching secular equilibrium (detailed methods are given in the supplemental data). To ensure identical radiolabeling levels (radioactivity-to-lipid ratio) across all liposome types, the levels of radioactivity introduced to the liposome suspension for encapsulation were adjusted in advance based on the loading efficacy measured for each liposome composition. Antibodies were radiolabeled following a published protocol described in detail in the supplemental data (*21*).

For ligand conjugation to liposomes, standard 3-(2-(pyridyldithio) propionate (PDP)–based and 1-ethyl-3(3-dimethylaminopropyl)carbodiimide (EDC)/*N*-hydroxysuccinimide (NHS)–based chemistry was followed to conjugate J591 antibodies and the A10 aptamers to liposomes, respectively (detailed methods are given in the supplemental data) (*22*).

Cell Lines

All cell lines (LnCaP, Mat-Lu, HUVEC, BT474, and MDA-MB-231) were acquired from American Type Culture Collection (ATCC) and were cultured in medium suggested by ATCC supplemented with 10% fetal bovine serum, penicillin (100 units/mL), and streptomycin (100 μg/mL) in an incubator at 37°C and 5% CO_2. F12K medium, used for HUVEC, was additionally supplemented with Heparin (Sigma-Aldrich) sodium salt (0.1 mg/mL) and endothelial cell growth supplement (ECGS) (0.03 mg/mL). To induce PSMA expression on HUVEC cells, monolayers of HUVEC on Matrigel (BD Biosciences) were exposed to MDA-MB-231 cell–conditioned media and were induced to express PSMA following a published method described in detail in the supplemental data (*20*).

Detection of Induced PSMA Expression on HUVEC by Immunofluorescence

PSMA expression induced on HUVEC was determined using J591-based immunofluorescence (a detailed protocol is given in the supplemental data) (*7*). The binding of rhodamine-labeled J591-conjugated liposomes to PSMA-expressing HUVEC cells after a 6-h incubation was imaged using an Olympus IX 70 inverted microscope with an exciter bandpass filter (540 ± 25 nm) and an emitter bandpass filter (605 ± 55 nm) (Chroma Technology Corp.).

Binding and Internalization of Liposomes by Cell Monolayers, Followed by Cytotoxicity Studies

Rhodamine-labeled liposomes were incubated with well-plated cells at a liposome-to-receptor ratio of 1-to-10 and 1-to-1. After

completion of incubation, cells were washed, scrapped, and suspended in phosphate-buffered saline. The fraction of liposomes bound to cells was quantified by measuring the fluorescence intensity of rhodamine corrected for potential light scattered by cells. The cell-internalized intensity was measured on cells treated with a stripping buffer (detailed methods are given in the supplemental data). These studies were repeated for the J591 antibody on all cell lines at the same antibody-to-receptor ratios.

To evaluate cytotoxicity, radioactivities ranging From 37×10^{-9} to 370 kBq/mL (10^{-9} to 10^{1} μCi/mL) were added to well-plated cell monolayers in a total final volume of 0.2 mL per well. At the end of incubation, cells were gently washed and were further incubated with sterile fresh complete medium (detailed methods are given in the supplemental data). Cell viability was evaluated using an (3-(4,5-dimethylthiazol-2-yl)-2,5-diphenyltetrazolium bromide assay (MTT assay). In parallel experiments, liposome-mediated radioactivity internalized by cells in monolayers was measured by cell trypsinization, followed by counting of the cell populations and associated radioactivities. For the radiolabeled antibody, cell-internalized radioactivity was calculated on the basis of measured immunoreactivity and extent of internalization.

Results are reported as the arithmetic mean of n independent measurements ± the SD. The Student *t* test was used to calculate significant differences in the behavior between the differently labeled liposomes for all cell lines studied. *P* values of less than 0.05 were considered to be significant.

RESULTS

Liposome Loading with ^{225}Ac, Conjugation of Anti-PSMA Ligands, and Vesicle Characterization

The loading efficiencies of ^{225}Ac into preformed liposomes were 58.0% ± 4.6% for liposomes with PDP-terminated PEG chains (L_P-PDP) and 85.6% ± 11.7% for liposomes with carboxyl-terminated PEG chains (L_P-COOH) ($n = 5$ independent loading experiments for each liposome type), and to facilitate comparison, all liposomes were prepared at the same radioactivity-to-lipid ratio. Antibody radiolabeling efficiency with ^{225}Ac ranged from 2.6% ± 0.2% to 3.0% ± 0.1%. The radioactivity that was stably retained by the J591 antibody was 86.7% ± 3.7% after a 24-h incubation in 10% serum-supplemented medium. The conjugation reaction resulted in 33 ± 4 μg of J591 antibody per 2.5 μmol of total lipid or approximately 17 ± 2 J591 antibodies per liposome ($n = 5$). For A10 aptamer, optimization of the conjugation reaction (Supplemental Fig. 1) resulted in 2.3 ± 0.5 μg of A10 aptamer per 2.5 μmol of total lipid or approximately 9 ± 2 A10 aptamers per liposome ($n = 5$). Ligand densities are calculated using the measured average size of liposomes of 107 ± 2 nm in diameter (polydispersity index, 0.07 ± 0.04). The immunoreactivities of radiolabeled J591 and of J591 conjugated on liposomes were 76.9% ± 2.7% and 21.3% ± 3.0%, respectively. Receptor blocking with unlabeled J591 antibody minimized cell association to 1.4% ± 0.2% and 1.1% ± 0.2%, respectively. The immunoreactivity of A10 aptamer conjugated on liposomes was 11.2% ± 1.0%, and receptor blocking by excess A10 aptamer decreased binding to 0.9% ± 0.8%. Specific binding was confirmed by lack of binding on PSMA-negative BT474 cells, which ranged from 0.2% ± 1.2% to 2.2% ± 0.3% for the antibody and all targeted constructs. Conjugation of J591 antibody or A10 aptamer did not result in measurable change in liposome size. Liposomes with and without conjugated anti-PSMA ligands exhibited similar retention of encapsulated ^{225}Ac at 6 h (72.8% ± 2.3%) and 24 h (69.4% ± 1.2%) in serum-supplemented medium ($n = 3$).

Induced Expression of PSMA on HUVEC and Binding of J591-Labeled Liposomes to PSMA-Expressing HUVEC

The micrographs shown in Supplemental Figure 2 illustrate that HUVEC cultured on Matrigel form tubular structures. However, detectable levels of PSMA expression—evaluated by binding of the anti-PSMA antibody J591—are confined only to HUVEC exposed to conditioned medium derived from MDA-MB-231 cells (Supplemental Fig. 2 on the bottom left, fluorescence image), in agreement with Liu et al. (*20*). Conjugation of J591 antibodies to liposomes does not affect the antibody's targeting selectivity. Supplemental Figure 3 shows that J591-labeled liposomes demonstrate enhanced binding to PSMA-expressing HUVECs relative to nontargeted liposomes, respectively.

Binding Selectivity of Liposomes to PSMA-Expressing Cell Monolayers

Flow cytometry detecting J591 cell surface association on all cell lines was used to evaluate the effective relative PSMA expression (Supplemental Fig. 4). With this method of measurement, LNCaP cells exhibit 2:1:0.5 greater PSMA expression relative to Mat-Lu and induced HUVEC, respectively. On the basis of this relative PSMA expression level, LNCaP and Mat-Lu were incubated with 2 different concentrations of liposomes corresponding to liposome-to-receptor ratios of 1:1 and 1:10. Because of experimental limitations imposed by the low number of harvested HUVEC cells, binding experiments on monolayers of HUVEC cells were conducted at only the ratio of 1:1 liposomes(or antibody) to receptors. The same liposome concentrations were used in incubations with A10 aptamer–labeled liposomes.

Table 1 illustrates that J591-labeled liposomes display higher levels of total specific binding to both LNCaP and Mat-Lu than A10 aptamer–labeled liposomes. The extent of specific binding of targeted liposomes is significant at 6 h and becomes more pronounced after 24 h of incubation. Table 1 shows a similar trend with respect to incubation time in the binding profile of J591-targeted liposomes to PSMA-expressing HUVEC whereby the total specific binding increases with incubation time. However, in contrast to LNCaP and Mat-Lu, the A10 aptamer–labeled liposomes do not show appreciable specific binding to PSMA-expressing HUVEC at either time point (<2.9%).

Table 1 also indicates that the LNCaP cell line exhibits approximately 26%–29% internalization of bound J591-labeled liposomes, which is essentially independent of the incubation time. J591-labeled liposomes are internalized at greater extents, 31%–35%, by Mat-Lu cells. Following the same trend, A10 aptamer–labeled liposomes are internalized to a greater extent by Mat-Lu cells (30%–36% at 24 h) than by LNCaP cells (25%–29%). Both J591-labeled liposomes and A10-labeled liposomes are internalized to a significant extent by PSMA-expressing HUVEC.

For comparison, J591 antibody exhibits on all cell lines and independent of incubation time greater extents of binding than any of the targeted liposomes. The extent of antibody internalization ranges between 27% and 38% of bound antibody.

At both time points, nontargeted liposomes display negligible association to LNCaP, Mat-Lu, and PSMA-expressing HUVEC (<1%, Supplemental Table 1). Both J591-labeled liposomes and A10 aptamer–labeled liposomes do not show specific binding to PSMA-negative cells (<1%).

TABLE 1
Specific Binding/Internalization of Targeted Liposomes and J591 Antibody by Cell Monolayers

			J591-labeled liposomes		A10 PSMA aptamer–labeled liposomes		J591 antibody	
Incubation time (h)	Cell line	Liposome or antibody:receptor ratio (Liposome or antibody:cell ratio)	% specifically bound and internalized liposomes	% specifically internalized liposomes (% internalized relative to bound liposomes)	% specifically bound and internalized liposomes	% specifically internalized liposomes (% internalized relative to bound liposomes)	% specifically bound and internalized antibody	% specifically internalized antibody (% internalized relative to bound antibody)
6	LnCaP	1:1 (18×10^4:1)	13.2 ± 1.4	3.6 ± 0.9 (27.2 ± 6.7)	7.2 ± 0.9	2.2 ± 0.7 (30.8 ± 10.5)	80.4 ± 6.3	30.6 ± 2.9 (38.1 ± 4.7)
		1:10 (18×10^3:1)	21.0 ± 2.8	5.5 ± 2.2 (26.2 ± 9.1)	10.2 ± 1.2	3.1 ± 1.1 (30.8 ± 12.1)	77.5 ± 3.3	42.7 ± 2.3 (33.5 ± 3.6)
	Mat-Lu	1:1 (9.6×10^4:1)	6.1 ± 1.1	1.9 ± 0.8 (30.6 ± 15.3)	5.4 ± 1.3	2.0 ± 0.1 (37.7 ± 8.3)	78.4 ± 3.1	26.3 ± 2.7 (33.5 ± 3.6)
		1:10 (9.6×10^3:1)	7.6 ± 2.3	2.7 ± 2.7 (35.9 ± 25.5)	8.0 ± 4.9	2.2 ± 0.1 (27.0 ± 8.7)	77.9 ± 5.2	39.4 ± 3.8 (27.0 ± 8.7)
	HUVEC (CCM + Matrigel)	1:1 (4.7×10^4:1)	5.2 ± 1.5	1.7 ± 0.3 (26 ± 17)	2.3 ± 0.4	0.6 ± 0.3 (25.8 ± 13.1)	27.1 ± 1.4	9.1 ± 0.5 (33.6 ± 2.4)
	BT474	— (13.8×10^4:1)	0.0 ± 0.9	— (—)	0.1 ± 0.1	— (—)	2.2 ± 0.7	— (—)
		— (13.8×10^3:1)	0.2 ± 1.2	— (—)	0.0 ± 1.4	— (—)	2.2 ± 0.3	— (—)
	HUVEC (Matrigel)	— (4.7×10^4:1)	0.5 ± 1.0	— (—)	1.0 ± 1.0	— (—)	3.3 ± 1.7	— (—)
	HUVEC	— (4.7×10^4:1)	0.5 ± 1.1	— (—)	0.4 ± 1.2	— (—)	2.5 ± 0.9	— (—)
24	LnCaP	1:1 (18×10^4:1)	17.3 ± 1.8	4.5 ± 1.2 (26.2 ± 6.0)	8.7 ± 1.3	2.5 ± 1.0 (29.1 ± 10.9)	72.6 ± 3.1	25.4 ± 1.8 (34.9 ± 2.9)
		1:10 (18×10^3:1)	26.2 ± 5.3	7.6 ± 3.8 (29.2 ± 10.2)	12.4 ± 4.9	3.1 ± 2.0 (25.1 ± 12.2)	73.0 ± 4.1	25.6 ± 3.5 (35.01 ± 5.2)
	Mat-Lu	1:1 (9.6×10^4:1)	8.4 ± 1.0	3.0 ± 0.9 (35.3 ± 12.0)	7.4 ± 1.3	2.5 ± 0.0 (36.0 ± 6.3)	73.4 ± 2.2	24.4 ± 2.7 (33.2 ± 3.7)
		1:10 (9.6×10^3:1)	11.2 ± 6.0	3.8 ± 2.4 (34.3 ± 17.4)	8.5 ± 4.6	2.6 ± 1.3 (30.8 ± 16.8)	73.9 ± 2.9	25.1 ± 1.4 (33.9 ± 2.3)
	HUVEC (CCM + Matrigel)	1:1 (4.7×10^4:1)	8.8 ± 2.2	2.3 ± 1.3 (23.2 ± 14.2)	3.2 ± 0.7	1.3 ± 0.3 (39.3 ± 12.7)	23.7 ± 2.5	10.9 ± 2.7 (28.6 ± 7.3)
	BT474	— (13.8×10^4:1)	−0.0 ± 0.1	—	0.1 ± 0.1	—	2.1 ± 0.9	—
		— (13.8×10^3:1)	−0.2 ± 1.6	—	0.0 ± 1.4	—	2.1 ± 1.3	—
	HUVEC (Matrigel)	— (4.7×10^4:1)	0.9 ± 0.9	—	0.7 ± 0.9	—	2.9 ± 0.6	—
	HUVEC	— (4.7×10^4:1)	0.4 ± 1.0	—	0.7 ± 1.1	—	1.9 ± 0.3	—

Specific binding is defined as extent of cell-bound targeted liposomes (or antibody) corrected for extent of nonspecifically bound nontargeted liposomes of same composition (or nonspecifically bound antibody in blocking studies by same nonlabeled antibody). Errors correspond to SD of 2 independent liposome preparations.

CCM = cell-conditioned media.

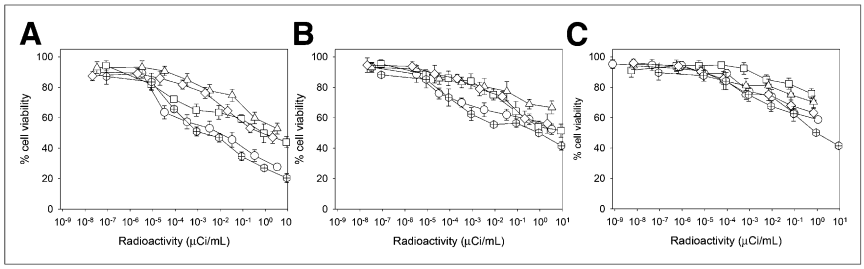

FIGURE 1. Toxicity of ^{225}Ac after 6-h incubation on PSMA-positive cell monolayers of LNCaP (A), Mat-Lu (B), and PSMA-expressing HUVEC (C). ^{225}Ac is encapsulated in J591-targeted liposomes (○), in A10 aptamer–labeled liposomes (□), in nontargeted liposomes (△), and in free chelated form (◇). Crossed hexagons are ^{225}Ac-labeled J591 antibody. Lines are guides to the eye. Error bars correspond to SD of repeated measurements (2 independent liposome preparations, 2 wells per run). 1 mCi = 37 MBq.

Cytotoxicity Profiles of ^{225}Ac-Loaded Liposomes

Cytotoxicity studies shown in Figures 1 and 2 demonstrate that J591-labeled liposomes loaded with ^{225}Ac are most cytotoxic, compared with other liposomal constructs tested on the PSMA-expressing LNCaP, Mat-Lu, and induced HUVEC (median lethal dose [LD_{50}] values are summarized in Table 2, $P < 0.05$ for most cases studied). The efficacy of J591-labeled liposomes, at the longer incubation times (24 h), is comparable ($P > 0.05$) to that of the radiolabeled J591 antibody. Radiolabeled A10 aptamer–labeled liposomes display higher cytotoxicity ($P < 0.05$) than nontargeted ^{225}Ac-loaded liposomes when compared on the LnCaP cell line.

On PSMA-negative BT-474 cells (Figs. 3A and 4A) and in HUVEC with no detectable PSMA expression (Figs. 3B, 3C, 4B, and 4C), there is no significant difference in cytotoxicity between any of the ^{225}Ac-loaded liposome constructs ($P > 0.05$).

Nontargeted liposomes and nonliposomal ^{225}Ac-DOTA exhibit some degree of cytotoxicity, which may be affected by their measured nonspecific partition on Matrigel (Supplemental Table 2). Liposomes not containing radionuclides were not cytotoxic (Supplemental Figs. 5 and 6).

DISCUSSION

In this study, we evaluated the potential of targeted liposomes loaded with the α-particle generator ^{225}Ac to selectively kill PSMA-expressing cells in the form of monolayers in vitro. The targeting ligands evaluated include the anti-PSMA antibody J591 (*7*) and the A10 PSMA aptamer (*9*), which are known to recognize the extracellular domain of the PSMA protein. The variability in PSMA expression by the human tumor neovasculature justifies the different cell lines used in this study. These include the highly expressing LNCaP cell line, with 180,000 copies per cell (*23*); the rat cell line Mat-Lu, which exhibits an almost 50% lower binding of the J591 antibody relative to LNCaP; and HUVEC monolayers induced to express PSMA (*20*) at, however, a significantly lower level (25% relative to LNCaP).

Our studies demonstrate the superiority of J591-labeled liposomes over both A10 PSMA-labeled liposomes and nontargeted liposomes in terms of their binding and internalization efficacies among all different cell lines and in terms of the observed LD_{50} values on cell monolayers for both incubation periods tested. A comparison between cell-associated radioactivity and cytotoxicity mediated by both types of targeted liposome constructs and the radiolabeled antibody demonstrates that the latter exhibits greater efficacy, closely followed by the antibody-targeted liposomes on the cell lines with lower PSMA expression (Fig. 5). Although on Figure 5, because of the experimental limitations only the internalized radioactivities per cell are presented, evaluation of the total cell-associated radioactivity would have resulted in similar trends since the measured extents of internalization for each modality are similar (Table 1) for a given cell line. The difference in efficacy of the 3 modalities could be potentially attributed to different intracellular trafficking; this would affect the intracellular localization and, therefore, the microdosimetry of the intracellularly emitted α particles given the subcellular range of α-particle trajectories (50–100 μm) and the potentially affected apparent diffusivities of the parent radionuclide and the emitted radioactive daughters (*24*).

The distributions of PSMA expression levels by endothelial tumor cells may vary (*5*), but for cases with moderate to low PSMA expression levels the above findings suggest that the J591-targeted liposomal approach to deliver ^{225}Ac, compared with the radiolabeled antibody approach, could overall be more or as efficacious despite an expected significant decrease in the binding affinity of J591-labeled liposomes relative to the J591 antibody alone (*25*). The rationale for this suggestion is 3-fold.

First, the specific activity of each carrier (defined here as radioactivity per delivery carrier; i.e., liposome vs. antibody) is significantly greater for liposomes than for the antibody. In particular, we have demonstrated that we can stably encapsulate up to three ^{225}Ac nuclides per every 2 liposomes (*18*). For comparison, the specific radioactivity for antibodies labeled with ^{225}Ac is reported to be as high as 2.22 kBq (60 nCi) per 0.3 μg of antibody, roughly corresponding to one ^{225}Ac per 435 antibodies (*26*). Using these protocols, we were able to prepare as high as 1.15 kBq (31 nCi) per 0.3 μg of antibody, roughly corresponding to one ^{225}Ac per 840 antibodies.

Second, particularly for ^{225}Ac, the potentially lower renal toxicities expected from a nanoparticle-based delivery approach—due to faster clearance—may en-

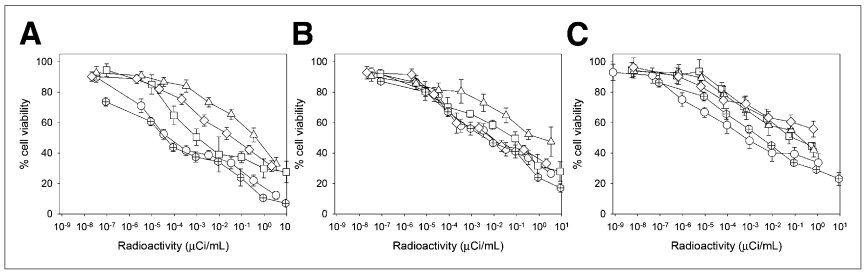

FIGURE 2. Toxicity of ^{225}Ac after 24-h incubation on PSMA-positive cell monolayers of LNCaP (A), Mat-Lu (B), and PSMA-expressing HUVEC (C). ^{225}Ac is encapsulated in J591-targeted liposomes (○), in A10 aptamer–labeled liposomes (□), in nontargeted liposomes (△), and in free chelated form (◇). Crossed hexagons are ^{225}Ac-labeled J591 antibody. Lines are guides to the eye. Error bars correspond to SD of repeated measurements (2 independent liposome preparations, 2 wells per run). 1 mCi = 37 MBq.

TABLE 2
LD_{50} Values of Liposome-Based Constructs and Radiolabeled J591 Antibody

Incubation time (h)	LD_{50} (Bq/mL [μCi/mL]). LNCaP	Mat-Lu	HUVEC
6			
J591-labeled liposomes	3.70×10^2 (1.0×10^{-2})	1.22×10^5 (3.3)	*
A10 aptamer–labeled liposomes	3.22×10^4 (8.7×10^{-1})	3.14×10^5 (8.5)	*
J591 antibody	5.92×10^1 (1.6×10^{-3})	3.29×10^4 (8.9×10^{-1})	3.28×10^4 (8.9×10^{-1})
Nontargeted liposomes	1.25×10^5 (3.4)	*	*
24			
J591-labeled liposomes	1.96 (5.3×10^{-5})	2.92×10^2 (7.9×10^{-3})	2.33×10^1 (6.3×10^{-4})
A10 aptamer- labeled liposomes	37 (1.0×10^{-3})	1.85×10^3 (5.0×10^{-2})	4.07×10^3 (1.1×10^{-1})
J591 antibody	1.37 (3.7×10^{-5})	1.52×10^2 (4.1×10^{-3})	1.11×10^2 (3.0×10^{-3})
Nontargeted liposomes	1.52×10^4 (4.1×10^{-1})	4.07×10^4 (1.1)	5.55×10^3 (1.5×10^{-1})

*LD_{50} not reached at highest concentration.

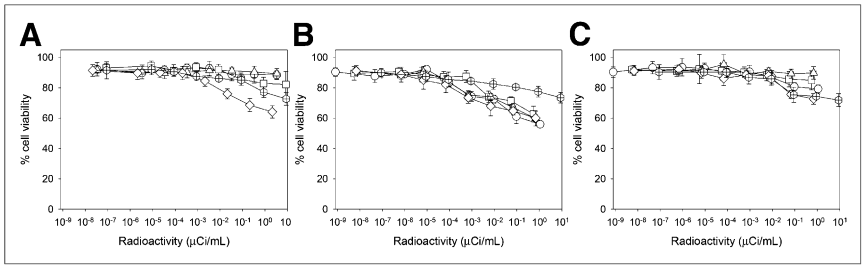

FIGURE 3. Toxicity of ^{225}Ac after 6-h incubation on PSMA-negative cell monolayers of BT474 (A), PSMA-negative HUVEC grown on Matrigel (B), and PSMA-negative HUVEC (C) grown in absence of Matrigel. ^{225}Ac is encapsulated in J591-targeted liposomes (○), in A10 aptamer–labeled liposomes (□), in nontargeted liposomes (△), and in free chelated form (◇). Crossed hexagons are ^{225}Ac-labeled J591 antibody. Lines are guides to the eye. Error bars correspond to SD of repeated measurements (2 independent liposome preparations, 2 wells per run). 1 mCi = 37 MBq.

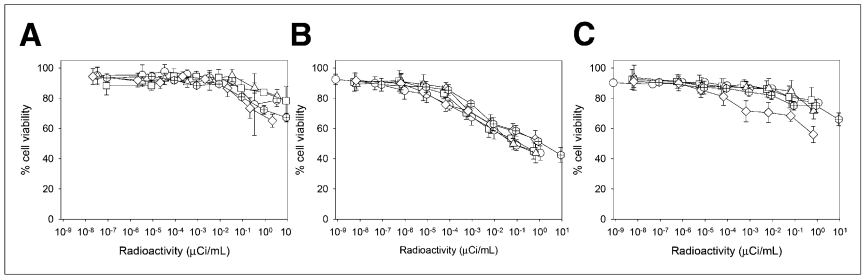

FIGURE 4. Toxicity of ^{225}Ac after 24-h incubation on PSMA-negative cell monolayers of BT474 (A), PSMA-negative HUVEC grown on Matrigel (B), and PSMA-negative HUVEC (C) grown in absence of Matrigel. ^{225}Ac is encapsulated in J591-targeted liposomes (○), in A10 aptamer–labeled liposomes (□), in nontargeted liposomes (△), and in free chelated form (◇). Crossed hexagons are ^{225}Ac-labeled J591 antibody (crossed hexagons). Lines are guides to the eye. Error bars correspond to SD of repeated measurements (2 independent liposome preparations, 2 wells per run). 1 mCi = 37 MBq.

able the liposomal approach to ultimately become a justifiable antivascular therapy. ^{225}Ac generates 3 α-particle–emitting daughters, and, during circulation, carriers loaded with ^{225}Ac cannot retain any of the daughters, increasing renal toxicity (*15*). Therefore, ^{225}Ac must be delivered at the tumor neovasculature using a strategy that combines fast binding to the target with rapid sequestration of ^{225}Ac-loaded carriers from the bloodstream and accumulation in less radiosensitive sites to spare radiosensitive organs from escaped daughters. Liposomes circulate for significantly shorter times in the blood, compared with antibodies, and therefore may result in a significant decrease in the cumulated radioactivity at the kidneys caused by escaped daughters occurring during circulation of ^{225}Ac. For example, liposomes can be engineered to exhibit half-lives on the order of 6 h by modifying their size and surface characteristics (*27*). This is significantly faster than the circulation half-lives of antibodies (*28*). In particular for J591, blood clearance in patients was reported to be described by a double exponential decay with a fast half-life of less than 3 h (for 20% of administered radioactivity) and with a slower half-life of 44 h (for 80% of administered radioactivity) (*29*). Therefore, for the same initial administered radioactivity A_o, the decrease of the average circulation half-life of the α-particle generator from several hours (when labeled on antibodies) to only a few hours (when encapsulated in liposomes) would roughly correspond to up to D = 81% decrease in the cumulated radioactivity ($\tilde{A}$) at the kidneys caused by escaped daughters, where $D = (\tilde{A}_{lipos} - \tilde{A}_{Ab}) \times 100/\tilde{A}_{Ab}$ and $\tilde{A}_{lipos} = A_o \times [(\ln 2/t^L{}_{1/2}) + (\ln 2/t^{rad}{}_{1/2})]\text{^}(-1)$ and $\tilde{A}_{Ab} = A_o \times [0.2 \times [(\ln 2/t^{Ab,f}{}_{1/2}) + (\ln 2/t^{rad}{}_{1/2})]\text{^}(-1) + 0.8 \times [(\ln 2/t^{Ab,s}{}_{1/2}) + (\ln 2/t^{rad}{}_{1/2})]\text{^}(-1)]$. ($\tilde{A}_{lipos}$ is the cumulated radioactivity at the kidneys caused by escaped daughters of ^{225}Ac encapsulated in liposomes and $\tilde{A}_{Ab}$ is the cumulated radioactivity at the kidneys caused by escaped daughters of ^{225}Ac labeled on antibodies.) This simplified calculation uses a single exponential function for the radioactive decay with $t^{rad}{}_{1/2}$ = 9.9 d for ^{225}Ac (*30*), a single exponential decay for the clearance of liposomes $t^L{}_{1/2}$ = 6 h, and a double exponential decay for

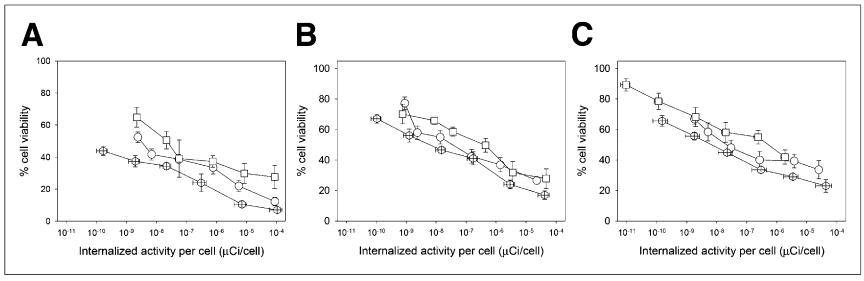

FIGURE 5. Cell viability as function of cell internalized radioactivity mediated by J591-labeled liposomes (○), A10 aptamer–labeled liposomes (□), and radiolabeled J591 antibody (crossed hexagons) after 24 h of incubation with LnCaP (A), MatLu (B), and PSMA-positive HUVEC monolayers (C). Lines are guides to the eye. Error bars correspond to SD of repeated measurements (2 independent liposome preparations, 2 wells per run). 1 mCi = 37 MBq.

antibodies with a fast ($t^{Ab,f}_{1/2}$ = 3 h) and a slow ($t^{Ab,s}_{1/2}$ = 44 h) decay weighted as reported (*29*).

Although the shorter circulation of liposomes is expected to also limit the actual extent of binding to the tumor endothelium, simultaneous liposome extravasation into the tumor interstitial space followed by retention within it enhanced permeability and retention effect (EPR effect) (*31*) may compensate for the delivered dose. Given the short penetration depths reported for nanometer-sized carriers (only 20–30 μm are reported for liposomes) (*32*) and the α-particle trajectories ranging from 50 to 100 μm, the extravasated liposomes would significantly contribute to the irradiation of the tumor vasculature.

Third, effective shift in the normal-organ toxicity of liposomes (liposome uptake) from the liver to the spleen can be achieved by just altering the size of the carrier without altering the preparation and loading protocols (*33*). The spleen, being less radiosensitive than the kidneys (*17*)—and although important to the defense of the body—could even be compromised under certain circumstances (*34–36*).

Finally, solely from geometric considerations, internalized α-particle emitters will have a higher probability to hit the nuclear DNA (*37,38*). Our studies demonstrate variable extents of internalization, which generally do not exceed approximately a third of specifically bound liposomes. Although these values are somewhat lower than the extent of internalization of the J591 antibody alone (Table 1 and (*23*)), as mentioned above, in an vivo setting, additional irradiation of the tumor endothelium by extravasated liposomes may compensate for lower liposome internalization.

This study demonstrates that anti-PSMA J591-labeled liposomes loaded with ^{225}Ac selectively target and kill cell monolayers with variable PSMA expression including PSMA-expressing HUVEC. Liposomes targeted with A10 PSMA aptamer seem promising for cell targets with relatively high PSMA expression. The approach of anti-PSMA liposomes loaded with ^{225}Ac, therefore, may provide a potential strategy for selective PSMA-targeting α radiotherapy.

CONCLUSION

This study evaluated the potential of targeted liposomes loaded with the α-particle generator ^{225}Ac to selectively kill PSMA-expressing human (LNCaP and HUVEC induced to express PSMA) and rat (Mat-Lu) cell lines in the form of monolayers in vitro. The targeting ligands evaluated include the anti-PSMA antibody J591 and the A10 PSMA aptamer, both recognizing the extracellular domain of the PSMA protein. J591-labeled liposomes exhibit cytotoxicities comparable to the radiolabeled J591 antibody, followed by the less cytotoxic A10 aptamer–labeled liposomes. The relatively low LD_{50} values of J591-labeled liposomes both on LNCaP and on PSMA-expressing HUVEC suggest the potential of these liposomes for selective antivascular α-radiotherapy.

DISCLOSURE

The costs of publication of this article were defrayed in part by the payment of page charges. Therefore, and solely to indicate this fact, this article is hereby marked "advertisement" in accordance with 18 USC section 1734. This study is supported by the Research Scholar grant RSG-12-044-01 from the American Cancer Society and in part by the National Science Foundation grant DMR1207022 and the Charles and Johanna Busch Memorial Fund. No other potential conflict of interest relevant to this article was reported.

REFERENCES

1. Folkman J. What is the evidence that tumors are angiogenesis dependent? *J Natl Cancer Inst.* 1990;82:4–6.
2. Folkman J. Tumor angiogenesis: therapeutic implications. *N Engl J Med.* 1971;285:1182–1186.
3. Burrows FJ, Thorpe PE. Eradication of large solid tumors in mice with an immunotoxin directed against tumor vasculature. *Proc Natl Acad Sci USA.* 1993;90:8996–9000.
4. Thorpe PE, Burrows FJ. Antibody-directed targeting of the vasculature of solid tumors. *Breast Cancer Res Treat.* 1995;36:237–251.
5. Chang SS, Reuter VE, Heston WDW, Bander NH, Grauer LS, Gaudin PB. Five different anti-prostate-specific membrane antigen (PSMA) antibodies confirm PSMA expression in tumor-associated neovasculature. *Cancer Res.* 1999;59:3192–3198.
6. Liu H, Moy P, Kim S, et al. Monoclonal antibodies to the extracellular domain of prostate-specific membrane antigen also react with tumor vascular endothelium. *Cancer Res.* 1997;57:3629–3634.
7. Liu H, Rajasekaran A, Moy P, et al. Constitutive and antibody-induced internalization of prostate-specific membrane antigen. *Cancer Res.* 1998;58:4055–4060.
8. Milowsky MI, Nanus DM, Kostakoglu L, et al. Vascular targeted therapy with anti-prostate-specific membrane antigen monoclonal antibody j591 in advanced solid tumors. *J Clin Oncol.* 2007;25:540–547.
9. Lupold SE, Hicke BJ, Lin Y, Coffey DS. Identification and characterization of nuclease-stabilized RNA molecules that bind human prostate cancer cells via the prostate-specific membrane antigen. *Cancer Research.* 2002;62:4029–4033.
10. Farokhzad OC, Cheng J, Teply BA, et al. Targeted nanoparticle-aptamer bioconjugates for cancer chemotherapy in vivo. *Proc Natl Acad Sci.* 2006;103:6315–6320.
11. Humm JL. A microdosimetric model of astatine-211 labeled antibodies for radioimmunotherapy. *Int J Radiat Oncol Biol Phys.* 1987;13:1767–1773.
12. Humm JL, Chin LM. A model of cell inactivation by alpha-particle internal emitters. *Radiat Res.* 1993;134:143–150.
13. Macklis RM, Kinsey BM, Kassis AI, et al. Radioimmunotherapy with alpha-particle-emitting immunoconjugates. *Science.* 1988;240:1024–1026.
14. Sgouros G, Roeske JC, McDevitt MR, et al. MIRD pamphlet No. 22 (abridged): radiobiology and dosimetry of α-particle emitters for targeted radionuclide therapy. *J Nucl Med.* 2010;51:311–328.
15. Miederer M, Scheinberg D, McDevitt M. Realizing the potential of the actinium-225 radionuclide generator in targeted alpha particle therapy applications. *Adv Drug Deliv Rev.* 2008;60:1371–1382.
16. Sofou S, Thomas JL, Lin H-Y, McDevitt MR, Scheinberg DA, Sgouros G. Engineered liposomes for potential α-particle therapy of metastatic cancer. *J Nucl Med.* 2004;45:253–260.
17. Goldenberg DM. Targeted therapy of cancer with radiolabeled antibodies. *J Nucl Med.* 2002;43:693–713.

18. Chang M-Y, Seideman J, Sofou S. Enhanced loading efficiency and retention of 225ac in rigid liposomes for potential targeted therapy of micrometastases. *Bioconjug Chem.* 2008;19:1274–1282.
19. Liu C, Huang H, Donate F, et al. Prostate-specific membrane antigen directed selective thrombotic infarction of tumors. *Cancer Res.* 2002;62:5470–5475.
20. Liu T, Jabbes J, Nedrow-Byers JR, Wu LY, Bryan JN, Berkman CE. Detection of prostate-specific membrane antigen on HUVECs in response to breast tumor-conditioned medium. *Int J Oncol.* 2011;38:1349–1355.
21. McDevitt MR, Ma D, Simon J, Frank RK, Kiefer GE, Scheinberg DA. Design and synthesis of actinium-225 radioimmunopharmaceuticals. *Appl Radiat Isot.* 2002;57:841–847.
22. Allen TM, Brandeis E, Hansen CB, Kao GY, Zalipsky S. A new strategy for attachment of antibodies to sterically stabilized liposomes resulting in efficient targeting to cancer cells. *Biochim Biophys Acta.* 1995;1237:99–108.
23. McDevitt MR, Barendswaard E, Ma D, et al. An alpha-particle emitting antibody ([^{213}Bi]J591) for radioimmunotherapy of prostate cancer. *Cancer Res.* 2000;60:6095–6100.
24. Palm S, Humm JL, Rundqvist R, Jacobsson L. Microdosimetry of astatine-211 single-cell irradiation: role of daughter polonium-211 diffusion. *Med Phys.* 2004; 31:218–225.
25. McQuarrie SA, Mercer JR, Syme A, Suresh MR, Miller GG. Preliminary results of nanopharmaceuticals used in the radiotherapy of ovarian cancer. *J Pharm Sci.* 2005;7:29–34.
26. Escorcia FE, Henke E, McDevitt MR, et al. Selective killing of tumor neovasculature paradoxically improves chemotherapy delivery to tumors. *Cancer Res.* 2010;70:9277–9286.
27. Sofou S. Surface-active liposomes for targeted cancer therapy. *Nanomedicine (Lond).* 2007;2:711–724.
28. Leveque D, Wisniewski S, Jehl FO. Pharmacokinetics of therapeutic monoclonal antibodies used in oncology. *Anticancer Res.* 2005;25:2327–2343.
29. Vallabhajosula S, Kuji I, Hamacher KA, et al. Pharmacokinetics and biodistribution of ^{111}In- and ^{177}Lu-labeled J591 antibody specific for prostate-specific membrane antigen: prediction of ^{90}Y-J591 radiation dosimetry based on ^{111}In or ^{177}Lu? *J Nucl Med.* 2005;46:634–641.
30. Pommé S, Marouli M, Suliman G, et al. Measurement of the ^{225}Ac half-life. *Appl Radiat Isot.* 2012;70:2608–2614.
31. Noguchi Y, Wu J, Duncan R, et al. Early phase tumor accumulation of macromolecules: a great difference between the tumor vs. normal tissue in their clearance rate. *Jpn J Cancer Res.* 1998;89:307–314.
32. Yuan F, Leunig M, Huang SK, Berk DA, Papahadjopoulos D, Jain RK. Microvascular permeability and interstitial penetration of sterically stabilized (stealth) liposomes in a human tumor xenograft. *Cancer Res.* 1994;54:3352–3356.
33. Moghimi S. Mechanisms of splenic clearance of blood cells and particles: towards development of new splenotropic agents. *Adv Drug Deliv Rev.* 1995; 17:103–115.
34. Borley N, ed. *Spleen*. London, U.K.: Elsevier; 2005.
35. Heniford BT, Park A, Walsh R, et al. Laparoscopic splenectomy in patients with normal-sized spleens versus splenomegaly: does size matter. *Am Surg.* 2001;67: 854–857.
36. Takemori N, Hirai K, Onodera R, Kimura S, Katagiri M. Durable remission after splenectomy for Waldenstrom's macroglobulinemia with massive splenomegaly in leukemic phase. *Leuk Lymphoma.* 1997;26:387–393.
37. Nikula TK, McDevitt MR, Finn RD, et al. Alpha-emitting bismuth cyclohexylbenzyl DTPA constructs of recombinant humanized anti-CD33 antibodies: pharmacokinetics, bioactivity, toxicity and chemistry. *J Nucl Med.* 1999;40: 166–176.
38. Chouin N, Bernardeau K, Davodeau F, et al. Evidence of extranuclear cell sensitivity to alpha-particle radiation using a microdosimetric model. I. Presentation and validation of a microdosimetric model. *Radiat Res.* 2009;171: 657–663.